

1 **Parameterization of a comprehensive explicit model for single-ring infiltration**

2

3 *Iovino M.^{1*}, Abou Najm M.R.², Angulo-Jaramillo R.³, Bagarello V.¹, Castellini M.⁴, Concialdi P.¹,*
4 *Di Prima S.⁵, Lassabatere L.³, Stewart R.D.⁶*

5

6 ¹ Department of Agricultural, Food and Forest Sciences, University of Palermo, Viale delle Scienze,
7 90128 Palermo, Italy

8 ² Department of Land, Air and Water Resources, University of California, Davis, CA 95616, United
9 States

10 ³ Université de Lyon; UMR5023 Ecologie des Hydrosystèmes Naturels et Anthropisés, CNRS,
11 ENTPE, Université Lyon 1, Vaulx-en-Velin, France

12 ⁴ Council for Agricultural Research and Economics - Agriculture and Environment Research Center
13 (CREA-AA), Via Celso Ulpiani 5, 70125 Bari, Italy

14 ⁵ Department of Agricultural Sciences, University of Sassari, Viale Italia, 39, 07100 Sassari, Italy

15 ⁶ School of Plant and Environmental Sciences, Virginia Polytechnic Institute and State University,
16 Blacksburg, VA, United State.

17 * Corresponding Author: massimo.iovino@unipa.it

18

19

20 **ABSTRACT**

21 Comprehensive infiltration models can simultaneously describe transient and steady-state
22 infiltration behaviors, and therefore can be applied to a range of experimental conditions. However,
23 satisfactory model accuracy requires proper parameterization, including estimating the transition
24 time from transient to steady-state flow conditions (τ_{crit}). This study focused on improving the
25 estimation of two parameters – τ_{crit} and a second constant called a – used in a comprehensive,
26 explicit, two-term model for single ring infiltration (hereafter referred to as the SA model).
27 Different studies have recommended that a should be as low as 0.45 to as high as 0.91.
28 Furthermore, τ_{crit} is often obtained a-priori by assuming that steady-state conditions are reached
29 before the end of an infiltration run. However, there has not been a systematic analysis of those
30 terms for different soils and infiltration conditions. To investigate these open issues related to the
31 use of the SA model, here we introduce a novel, iterative method for estimating τ_{crit} and the
32 parameter a . We then applied this method to both analytical and experimental infiltration data, and
33 compared it with two existing empirical methods. The analytical infiltration experiments showed
34 that τ_{crit} was approximately 1.5 times larger than the maximum validity time of a similar two-term

35 transient infiltration model. Further, the iterative method for obtaining τ_{crit} had minimal effects on
36 the a term, which varied between 0.706 and 0.904 and was larger for finer soils and when small
37 water sources were used. Application of the proposed method was less efficient with experimental
38 data. Only ~33% of the experiments yielding plausible estimates of a (i.e., $a < 1$), indicating that
39 these infiltration model parameters often have high uncertainty. The successful runs indicated that a
40 depended on the rate at which the initial infiltration rate approached the final infiltration rate.
41 Depending on the fitting algorithm used, a had mean values of 0.74 – 0.78, which were intermediate
42 between those suggested by previous studies. Altogether, these findings expand the applicability of
43 the SA model by providing new methods for estimating τ_{crit} and by showing that a does not need to
44 be fixed a-priori. We expect that these advances will result in more reliable estimations of soil
45 hydrodynamic parameters, including hydraulic conductivity.

46

47 Keywords: Single ring infiltrometer, infiltration model parameterization, transition time

48

49 INTRODUCTION

50 Field infiltration experiments are often used to determine soil saturated hydraulic conductivity, K_s ,
51 or near-saturated variations with minimum disturbance to the sampled soil volume (Angulo-
52 Jaramillo et al., 2016; Bouma, 1982). Single ring infiltration tests offer the advantages of being easy
53 to conduct and requiring minimal and inexpensive equipment. Three-dimensional flow from a
54 single ring can be simulated by numerically solving the axisymmetric Richards equation with finite
55 element codes (e.g., Šimůnek et al., 2018). However, estimating soil hydraulic parameters from
56 numerical inversion of infiltrometer experiments is cumbersome and may experience a number of
57 problems related to computational efficiency, convergence, and parameter uniqueness (Lazarovitch
58 et al., 2007; Russo et al., 1991). Explicit solutions that account for three-dimensional flow paths in
59 the soil are thus preferred for interpreting infiltration from a single ring source (Dohnal et al., 2016;
60 Smith et al., 2002). Many formulations describe three-dimensional flow using the so-called α^*
61 parameter, which is often considered the reciprocal of soil macroscopic capillary length, λ ,
62 (Reynolds and Elrick, 2002).

63 At the same time, infiltration solutions need to account for the different phases of typical infiltration
64 processes, which progress from an initial transient phase to a subsequent steady-state phase. Some
65 models, e.g., Reynolds and Elrick (1990), determine K_s from three-dimensional, steady, ponded
66 flow out of the ring. These approaches require reliable steady-state infiltration rate data, which can
67 be impractical in some cases if the equilibration time is particularly long (Bagarello et al., 2019). By
68 contrast, models that make use of the transient stage of the infiltration process overcome

69 uncertainties about the time at which steady-state flux is attained. Their interpretation allows for
70 shorter experiments and smaller sampled volumes of soil, which provides better agreement with the
71 hypotheses of homogeneity and initial uniform water content assumed by infiltration models (Di
72 Prima et al., 2016; Vandervaere et al., 2000). However, these transient approaches require accurate
73 measurement in the early stage of infiltration, which can be challenging under specific field
74 conditions such as highly permeable, slightly sorptive and water-repellent soils (Di Prima et al.,
75 2019).

76 The limitations associated with models focused exclusively on transient or steady-state behaviors
77 has led to the development of several comprehensive models that can be applied under different
78 infiltration stages (i.e. from early time to steady state conditions) and various initial and boundary
79 conditions at the soil surface. One of the earliest comprehensive models for three-dimensional
80 cumulative infiltration, I , vs. time, t , from a disk source into an initially unsaturated soil was
81 proposed by Haverkamp et al. (1994). This solution is valid for any infiltration time, but can be
82 complex to apply due to its implicit form. Its explicit expansions, valid for transient and steady-state
83 infiltration stages, have successively been applied in a procedure known as Beerkan Estimation of
84 Soil Transfer (BEST) parameters (Lassabatere et al., 2006), which allows a complete soil hydraulic
85 characterization from a single ring infiltration test complemented by some basic soil physical
86 characterization. One limitation of the Haverkamp model is that it was developed for tension
87 infiltrometers, where the surface pressure head is less than or equal to zero and the disk source rests
88 on the soil surface, making it less accurate in situation where source pressure head or ring insertion
89 depths are positive (Stewart and Abou Najm, 2018a). The Haverkamp model also is only strictly
90 valid under relatively dry initial soil water contents, i.e. the ratio of initial soil water content to
91 saturated water content below 0.25.

92 Wu et al. (1999) proposed a generalized solution to infiltration from single-ring pressure
93 infiltrometers which removed the requirements of steady-state and allowed estimation of K_s from
94 the whole $I(t)$ curve without assuming a pre-established value of the soil macroscopic capillary
95 length or α^* parameter. Building on the Wu et al. (1999) and Reynolds and Elrick (1990) solutions,
96 Stewart and Abou Najm (2018a,b) developed a comprehensive infiltration model (SA model) for
97 single ring source that appears to be particularly flexible as compared to other models. Specifically,
98 it accounts for different ring sizes and depths of insertion, initial water contents, transient and
99 steady-state infiltration behavior, and non-zero water supply pressures. However, the SA model
100 uses a scaling parameter, referred to “ a ”, whose exact value is subject to some debate. For example,
101 Wu and Pan (1997) fitted a dimensionless infiltration equation to the numerically simulated single-
102 ring infiltration data for three representative soils (sand, clay, sandy-clay-loam) and obtained $a =$

103 0.91, a value that was subsequently used in an infiltration model by Wu et al. (1999). By analogy
104 with Philip (1990), Stewart and Abou Najm (2018a) suggested that a should instead be equal to
105 0.45, i.e., approximately one half of the value recommended by Wu and Pan (1997). Those authors
106 included a sensitivity analysis as on the a parameter, which showed that a varies between different
107 soil types and initial water contents. These different recommendations and results imply that the a
108 parameter warrants further investigation.

109 At the same time, application of either the SA model or the Haverkamp model requires estimates
110 for the timescales over which the transient infiltration solutions are valid. In the SA model, the
111 transition time is defined by τ_{crit} , which was specified by Stewart and Abou Najm (2018a) to ensure
112 continuity in the expressions for both infiltration rates and cumulative infiltration amounts. The
113 Haverkamp model defines a slightly different term t_{max} , which represents the maximum time over
114 which the transient solution applies. Both terms can be analytically defined (see Theory), and
115 moreover, for null pressure head at the infiltration surface and depth of ring insertion equal to zero,
116 the SA model and the explicit expansion of the Haverkamp model describe the same process and,
117 thus, can be compared to identify the relationship between τ_{crit} and t_{max} .

118 Identifying τ_{crit} and t_{max} based on infiltration measurements poses a related set of challenges, as the
119 parameters required to estimate these timescales are typically unknown a-priori. Assuming the
120 steady-state conditions are reached before the end of an infiltration run, Di Prima et al. (2019)
121 estimated the transition time as the first value for which linear regression line conducted for the last
122 three $I(t)$ data points deviates from the measured cumulative infiltration by a fixed threshold, often
123 fixed at 2% following Bagarello et al. (1999). This approach may introduce considerable
124 uncertainty in cases where steady-state conditions have not actually been met, thus warranting more
125 study of this estimation approach. Furthermore, this method may identify τ_{crit} values, and by
126 extension infiltration model parameters, that violate the requirement that infiltration rate be
127 continuous between the transient and steady-state phases.

128 This study investigates three open issues related to the use of the SA model for single ring
129 infiltration: 1) how comparable is τ_{crit} with the maximum time, t_{max} ? 2) how sensitive is τ_{crit} to the
130 empirical criterion used to fit it? 3) how does the scaling parameter a depend on different
131 experimental conditions and can it be related to the parameters of Haverkamp model? To answer
132 these questions, we applied an optimization procedure with a constraint among the infiltration
133 coefficients to fit the SA model to both analytical and experimental infiltration data. We used that
134 procedure to derive τ_{crit} and the associated value of a for each infiltration process. The outcomes of
135 proposed approach, which involves a simultaneous and coherent use of both transient and steady-

136 state infiltration data, is then discussed on the basis of theoretical considerations and comparison
 137 with simplified approaches to estimate the transition time.

138

139 THEORY

140

141 Infiltration model

142 Stewart and Abou Najm (2018a), building on the Wu et al. (1999) and Reynolds and Elrick (1990)
 143 solutions, developed the following explicit expressions of transient and steady-state three-
 144 dimensional (3D) cumulative infiltration, I (L), from a surface circular source under a positive
 145 pressure head:

$$146 \quad I = \sqrt{\frac{(\theta_s - \theta_i)(h_{source} + \lambda)K_s}{b}} \sqrt{t} + a f K_s t \quad t < \tau_{crit} \quad (1a)$$

$$147 \quad I = \frac{(\theta_s - \theta_i)(h_{source} + \lambda)}{4 f b (1 - a)} + f K_s t \quad t \geq \tau_{crit} \quad (1b)$$

$$148 \quad \tau_{crit} = \frac{(\theta_s - \theta_i)(h_{source} + \lambda)}{4 b K_s f^2 (1 - a)^2} \quad (1c)$$

149 where t (T) is the time, τ_{crit} (T) is the time of transition between early-time and steady-state
 150 infiltration behaviors, θ_s ($L^3 L^{-3}$) and θ_i ($L^3 L^{-3}$) are the respective saturated and initial volumetric
 151 soil water contents, h_{source} (L) is the established ponded depth of water on the infiltration surface, λ
 152 (L) is the macroscopic capillary length of the soil, K_s ($L T^{-1}$) is the saturated soil hydraulic
 153 conductivity, a and b are dimensionless constants (with $b \approx 0.55$; White and Sully, 1987), and f is a
 154 dimensionless correction factor that depends on soil initial and boundary conditions and ring
 155 geometry:

$$156 \quad f = \frac{h_{source} + \lambda}{d + r_d / 2} + 1 \quad (2)$$

157 where d (L) is the depth of ring insertion and r_d (L) is the radius of the ring. The macroscopic
 158 capillary length, λ , is a measure of the soil capillary force. It is defined as the matrix flux potential,
 159 ϕ ($L^2 T^{-1}$), scaled by the difference between K_s and the soil hydraulic conductivity, K_i ($L T^{-1}$),
 160 corresponding to the initial soil water pressure head, h_i (L):

$$161 \quad \lambda = \frac{\phi}{\Delta K} = \frac{1}{K_s - K_i} \int_{h_i}^0 K(h) dh \quad (3).$$

162 Larger values of λ indicate greater contribution of the capillary forces relative to gravity. The τ_{crit}
 163 time in Eq.(1c) is defined as the time when the infiltration rate (dI/dt) is equal between Eqs.(1a) and
 164 (1b).

165 A general form of Eq.(1) can be written as follows:

$$166 \quad I = c_1\sqrt{t} + c_2t \quad t < \tau_{crit} \quad (4a)$$

$$167 \quad I = c_3 + c_4t \quad t \geq \tau_{crit} \quad (4b)$$

$$168 \quad \tau_{crit} = \frac{1}{4} \left(\frac{c_1}{c_4 - c_2} \right)^2 \quad (4c)$$

169 where the infiltration coefficients c_1 ($L T^{-0.5}$) and c_2 ($L T^{-1}$) can be determined by fitting Eq.(4a) to
 170 the data corresponding to the transient time, and the intercept, c_3 (L), and the slope, c_4 ($L T^{-1}$), of
 171 Eq.(4b) can be estimated by linear regression analysis of the I vs. t data points associated with
 172 steady-state conditions. To ensure continuity of cumulative infiltration, I , between Eqs.(4a) and (4b)
 173 at $t = \tau_{crit}$, the following constraint should be placed among the four infiltration coefficients:

$$174 \quad c_3 = \frac{c_1^2}{4(c_4 - c_2)} = \tau_{crit} (c_4 - c_2) \quad \text{with } c_4 > c_2 \quad (5).$$

175 Here, we propose a novel and simple method for direct estimation of a from a single-ring
 176 experiment that includes both the transient and the steady-state phases of the infiltration process. In
 177 particular, the a constant can be derived from the parameterization of the infiltration coefficients c_2
 178 and c_4 via:

$$179 \quad \frac{c_2}{c_4} = \frac{a f K_s}{f K_s} = a \quad (6).$$

180 The a constant thus quantifies the weight of conductivity part of infiltration equation in the transient
 181 state (c_2) as a proportion of that in the steady state condition (c_4). Note that the condition $c_4 > c_2$,
 182 stated in Eq.(5), indicates that a should be < 1 to be physically plausible or that the conductivity
 183 weight is higher at the steady state than under transient conditions.

184

185 **Investigation of $a=c_2/c_4$ ratio with the approach by Haverkamp et al. (1994)**

186 Haverkamp et al. (1994) proposed a set of two-term expansions for transient and steady-state
 187 infiltration from a circular source, which are conceptually and functionally similar to Eqs.(1a) and
 188 (1b):

$$189 \quad I(t) = c_1\sqrt{t} + c_2t = S\sqrt{t} + \left(\frac{2-\beta}{3} \Delta K + K_i + \frac{\gamma S^2}{r_d \Delta \theta} \right) t \quad t < t_{max} \quad (7a)$$

$$190 \quad I(t) = c_3 + c_4t = \frac{1}{2(1-\beta)} \ln \left(\frac{1}{\beta} \right) \frac{S^2}{\Delta K} + \left(K_s + \frac{\gamma S^2}{r_d \Delta \theta} \right) t \quad t > t_{max} \quad (7b)$$

191 in which S ($L T^{-1/2}$) is the soil sorptivity, β and γ are infiltration constants that are usually fixed at β
 192 $= 0.6$ and $\gamma = 0.75$, and t_{max} (T) is the maximum time for which the transient expansion can be
 193 considered valid (Lassabatere et al., 2006). Unlike the SA model, however, the two expressions of

194 Eq.(7) asymptotically approach the quasi-exact infiltration solution but are not considered valid at t
 195 $= t_{max}$. Thus, a discontinuity between the two equations is expected at $t = t_{max}$ (Lassabatere et al.,
 196 2009; Angulo-Jaramillo et al., 2019). Nonetheless, this formulation is useful for exploring the
 197 validity of estimating a based on the ratio of the infiltration terms that scale linearly with time t .
 198 Specifically, substituting coefficients c_2 and c_4 of Eq.(7) into Eq.(6), and using the White and Sully
 199 (1987) expression for S , the following relationship for a is obtained:

$$200 \quad a = \frac{\left(\frac{2-\beta}{3}\Delta K + K_i + \frac{\gamma\lambda}{br_d}\right)}{\left(K_s + \frac{\gamma\lambda}{br_d}\right)} \quad (8).$$

201 Assuming that $K_i \approx 0$, which is the case for most applications of the model (when $\theta_i \leq 0.25 \theta_s$),
 202 and considering that Stewart and Abou Najm (2018a) showed that λ remained constant with $\lambda \approx$
 203 λ_{max} for initial degrees of saturation lower than 0.4, the following expression for a can be obtained:

$$204 \quad a = \frac{\left(\frac{2-\beta}{3}K_s + \frac{\gamma\lambda_{max}}{br_d}\right)}{\left(K_s + \frac{\gamma\lambda_{max}}{br_d}\right)} \quad (9).$$

205 Eq.(9) shows that the value of a depends on the soil type (K_s , λ_{max}) and ring radius (r_d), as well as
 206 on the values of the infiltration constants β and γ . In particular, for small ring radii or soils with high
 207 capillarity (e.g., fine-textured soils), the term $\gamma\lambda_{max}/br_d$ dominates in both the numerator and
 208 denominator, causing a to tend towards 1. Note that this maximum value of a is very close to $a =$
 209 0.91 suggested by Wu and Pan (1997) from numerical simulations conducted on differently textured
 210 soils. Conversely, for large rings or coarse soils, the first term dominates in both the numerator and
 211 the denominator and a tends towards $\frac{2-\beta}{3}$, which equals 0.467 for $\beta = 0.6$. In a similar way, for a
 212 given soil, as r_d increases, the contribution of the lateral capillarity decreases and the flow is
 213 dominated by gravity resulting in a decreasing a value that again approaches $\frac{2-\beta}{3} = 0.467$ (for $\beta =$
 214 0.6) as $r_d \rightarrow \infty$. Note that this minimum value of a is very close to $a = 0.45$ suggested by Stewart
 215 and Abou Najm (2018a) based on analogy with 1D infiltration. Overall, this analysis shows that a
 216 cannot be considered a constant regardless of soil type and experimental conditions, but instead
 217 represents a scale parameter between transient and steady infiltration rates for a single ring three-
 218 dimensional infiltration process.

219

220 **Investigation of τ_{crit} with the approach by Haverkamp et al. (1994) and Lassabatere et al.** 221 **(2006)**

222 On the basis of the approximate expansions defined by Haverkamp et al. (1994), Lassabatere et al.
 223 (2006) defined the maximum time t_{max} involved in Eq.(7) as the time that separates the transient
 224 from the steady states. These authors specifically evaluated t_{max} by differentiating Eq.(7), which

225 showed that the transient infiltration rate, $q_{tst}(t)$, decreases from infinity to $q_{tst,+\infty} = \frac{2-\beta}{3} \Delta K +$
 226 $K_i + \frac{\gamma S^2}{r_d \Delta \theta}$, whereas the steady state infiltration rate, $q_{sst}(t)$, remains constant at $q_{+\infty} = K_s + \frac{\gamma S^2}{r_d \Delta \theta}$.
 227 Since $q_{tst,+\infty} < q_{+\infty}$, there is a time for which the transient infiltration rate $q_{tst}(t)$ equals $q_{+\infty}$,
 228 which allows t_{max} to be defined as follows:

$$229 \quad t_{max} = \frac{1}{4(1-B)^2} \left(\frac{S}{K_s} \right)^2 \quad (10)$$

230 in which $(S/K_s)^2$ is the gravity time (t_{grav}) defined by Philip (1969), and where:

$$231 \quad B = \frac{2-\beta}{3} \frac{\Delta K}{K_s} + \frac{K_i}{K_s} \approx \frac{2-\beta}{3} \quad (11).$$

232 Note that the approximation $B = \frac{2-\beta}{3}$ accounts for the fact that $K_i \ll K_s$ when $\theta_i \ll \theta_s$. This
 233 remains the case for most initial water contents that fulfill the assumption of validity of
 234 Haverkamp's model, i.e., $\theta_i \leq 0.25 \theta_s$.

235 The determination of t_{max} on the basis of infiltration rates is similar to the definition of τ_{crit} by
 236 Stewart and Abou Najm (2018a,b). Here we simplify their expression by using the White and Sully
 237 (1987) equation for sorptivity and considering the case of a Beerkan test, i.e., a zero water pressure
 238 head at surface and a shallow depth of ring insertion ($h_{source} = 0$; $d = 0$). Under these conditions,
 239 Eq.(1c) can be written as:

$$240 \quad \tau_{crit} = \frac{1}{4f^2(1-a)^2} \frac{K_s}{\Delta K} \left(\frac{S}{K_s} \right)^2 \approx \frac{1}{4f^2(1-a)^2} \left(\frac{S}{K_s} \right)^2 \quad (12).$$

241 Finally, comparing Eqs.(10) and (12) we arrive at the following relationship between τ_{crit} and t_{max} :

$$242 \quad \tau_{crit} = \frac{(1-B)^2}{f^2(1-a)^2} t_{max} \quad (13).$$

243 Thus, the two characteristic times (τ_{crit} and t_{max}) are related by a proportionality constant that
 244 depends on soil properties and initial conditions as well as ring radius.

245

246 MATERIALS AND METHODS

247 Both analytically generated and field measured infiltration data were used in this investigation
 248 [dataset] (Iovino et al., 2021). The former data were used to exclude experimental errors while the
 249 latter ones were considered since the infiltration model is oriented towards field use.

250

251 Analytically generated infiltration data

252 Infiltration data were analytically generated with the 3D implicit model of Haverkamp et al. (1994)
 253 to obtain estimates of τ_{crit} and a for ideal soil conditions (error-free synthetic data). A total of 144
 254 Beerkan infiltration runs were modeled for the six soils (sand, loamy sand, sandy loam, loam, silt

255 loam and silty clay loam), which were considered by Hinnell et al. (2009) to cover a wide range of
256 hydraulic responses. The parameters by Carsel and Parrish (1988) were used to describe the water
257 retention curve and the hydraulic conductivity function of these soils according to the van
258 Genuchten-Mualem model (van Genuchten, 1980). The infiltration parameters were set at the
259 recommended values of $\beta = 0.6$ and $\gamma = 0.75$ (Haverkamp et al., 1994; Smettem et al., 1994). The
260 question of this choice of β and γ was investigated by Lassabatere et al. (2009), who compared the
261 implicit infiltration model of Haverkamp et al. (1994) with a numerical solution of Richards'
262 equation. They showed that a specific calibration of infiltration parameters can improve prediction
263 of cumulative infiltration. However, using the default values of infiltration parameters did not
264 compromise estimation of S and K_s obtained by inverting the implicit model (Latorre et al., 2018).
265 The initial water content was calculated based on the degree of saturation, S_e , where $S_e = (\theta_i -$
266 $\theta_r)/(\theta_s - \theta_r)$ and θ_i , θ_r and θ_s represent the respective initial, residual and saturated volumetric soil
267 water contents. The model was run with S_e values of 0.1, 0.2, 0.3, 0.4, 0.5, 0.6, 0.7 and 0.8, with
268 three ring radii of $r_d = 40, 75$ and 150 mm simulated for each S_e value. We note that previous work
269 has recommended that values of θ_i/θ_s should not exceed 0.25 for Eqs.(7) and (8) to remain valid
270 (Lassabatere et al., 2006, Lassabatere et al., 2009); however, wetter conditions often occur in
271 practice (Di Prima et al., 2016) and, therefore, it makes sense to test the analytical models under
272 these conditions. The duration of each run was fixed at $3 \times t_{max}$, with t_{max} calculated according to
273 Eq.(10), to obtain data for both the transient and the steady-state phases of the infiltration process.
274 Each simulation consisted of 50 $I(t)$ data pairs. Other details on the simulation procedure can be
275 found in Bagarello et al. (2017).

276 In this study, we used an iterative procedure to find the optimal set of infiltration coefficients $c_1, c_2,$
277 c_3, c_4 and their associated τ_{crit} value. This method consisted of fixing a tentative time, t_j , to separate
278 transient ($t < t_j$) and steady-state ($t \geq t_j$) conditions. Then, c_1, c_2 and c_4 were estimated by fitting
279 Eqs.(4a) and (4b) to the data with c_3 defined by Eq.(5). The corresponding $\tau_{crit,j}$ value was then
280 calculated by Eq.(4c) and the absolute difference between t_j and $\tau_{crit,j}$ is determined. The procedure
281 was repeated for a range of t_j values. The optimal parameter values were then identified as those
282 yielding the minimum value, i.e., $\min(|t_j - \tau_{crit,j}|)$.

283 For each infiltration run, 40 iterations were conducted with t_j time starting from the fifth $I(t)$ data
284 point and ending at the 45th $I(t)$ data point. This choice allowed a minimum infiltration dataset of
285 five points to fit either the transient or the steady-state stage of the infiltration process. For a
286 tentative time, t_i , linear regression was applied to fit Eq.(4b) to steady-state infiltration data ($t \geq t_j$).
287 The fitting of Eq.(4a) to the transient infiltration data ($t < t_j$) was conducted with a non-linear least

288 squares optimization technique that minimized the squared differences between measured and
 289 predicted cumulative infiltration (Vandervaere et al., 2000; Lassabatere et al., 2006). Such approach
 290 was hereinafter indicated as criterion IT-CI (transient cumulative infiltration data fitted by non-
 291 linear least squares technique). To explore the influence of the fitting technique on the estimation of
 292 coefficients c_1 and c_2 , a second optimization procedure was conducted using the cumulative
 293 linearization technique proposed by Smiles and Knight (1976) (criterion IT-CL). The main
 294 characteristics of the different criteria for applying the SA model to the infiltration data are
 295 summarized in **Table 1**.

296 The maximum error, E_{max} , normalized by the final cumulative infiltration, was determined using:

$$297 \quad E_{max} = \max \frac{|I_{opt} - I|}{I_f} \quad (14)$$

298 where I_{opt} is the cumulative infiltration estimated by Eqs.(4a) and (4b) with the optimal set of
 299 coefficients, I is the corresponding analytically calculated value, and I_f is cumulative infiltration at
 300 the end of simulation (i.e., $t = 3 \times t_{max}$). Using the optimal set of coefficients, the a constant was
 301 calculated by Eq.(6). The transition time, τ_{crit} , estimated by the iterative procedure was compared to
 302 t_{max} to evaluate proportionality between the two characteristic times.

303 We also conducted a sensitivity analysis of a values estimated by the iterative criterion by fixing
 304 τ_{crit} at t_{max} (i.e., one third of the total duration of the experiment, since modelling was performed for
 305 time up to $3 t_{max}$). Eq.(4a) was fitted to the transient ($t < t_{max}$) data by a non-linear least squares
 306 optimization technique and Eq.(4b) was fitted to steady-state ($t \geq t_{max}$) portions of the run by linear
 307 regression. The scaling parameter a was then calculated from Eq.(6).

308

309 **Field experiment**

310 Two Sicilian soils were chosen for this investigation. A loam soil (AR site) was located at the
 311 Department of Agricultural, Food and Forest Sciences of the Palermo University (Italy). A silty-
 312 clay soil (RO site) was located near Roccamena, approximately 70 km south of Palermo. The AR
 313 soil supported a citrus orchard under no tillage. The RO soil supported a fruit orchard under no
 314 tillage. Soil at the AR site was sampled on five different dates (November 2017, April, May and
 315 September 2018, April 2019) to encompass a range of environmental conditions. Soil was sampled
 316 only once at RO sites (June 2019). The same experimental protocol was applied for each of the
 317 overall six sampling campaigns.

318 For each sampling campaign, 10 infiltration runs were carried out at randomly selected locations
 319 within a bare area of approximately 150 m². At each infiltration site, the sampled soil surface was
 320 gently leveled and smoothed by manual implements. Small diameter (0.08 m) rings were inserted

321 on the soil surface to a depth of 0.01 m following the Beerkan infiltration procedure (Lassabatere et
 322 al., 2006). Ring insertion was conducted manually by gently using, if necessary, a rubber hammer,
 323 while ensuring that the upper rim of the ring remained horizontal during insertion. Then, 30 water
 324 volumes, each of 57 mL, were successively poured onto the confined infiltration surface. A
 325 relatively large cumulative infiltration height (approximately 0.34 m of water) was used to attain
 326 quasi-steady state conditions. For each water volume, the infiltration time was measured from water
 327 application to disappearance of all water, when the subsequent water volume was poured on the
 328 infiltration surface. Water was applied at a small distance from the infiltration surface, i.e.,
 329 approximately at a height, h_w , of 0.03 m, with the practitioner's fingers used to dissipate the kinetic
 330 energy of the falling water and thereby minimize soil disturbance due to water application. After the
 331 infiltration test, two undisturbed soil cores (0.05 m in height by 0.05 m in diameter) were collected
 332 nearby at 0 to 0.05 m and 0.05 to 0.10 m depths. These cores were used to determine the dry soil
 333 bulk density, ρ_b , and the initial soil water content, θ_i . The data were averaged over the two depths
 334 and paired with the corresponding infiltration run (**Table 2**).

335 The iterative criterion set up for analytical data (IT-CI) was also applied to field data to
 336 simultaneously estimate the infiltration coefficients (c_1 , c_2 , c_3 , and c_4 , with c_3 constrained by Eq.5),
 337 the transition time, and the related a value.

338 In addition to the above procedure, we also tested a more practical approach to fit the SA model to
 339 the infiltration data. We first split the cumulative infiltration for each run into transient versus
 340 steady state, specifically by estimating the transition time, τ_{crit} , according to the empirical criterion
 341 proposed by Di Prima et al. (2019). We presumed that steady-state conditions were reached before
 342 the end of the run, where the total run corresponded to N_{tot} data points, and then carried out a linear
 343 regression analysis on the last n data pairs (t_i, I_i) $i \in \{N_{tot}-n+1, \dots, N_{tot}\}$. Then, we computed the
 344 relative error between the regression line $I_{reg,n}(t_i)$ and the observed cumulative infiltration $I(t_i)$:

$$345 \quad \hat{E}(n) = \left| \frac{I(t_{N_{tot}-n+1}) - I_{reg,n}(t_{N_{tot}-n+1})}{I(t_{N_{tot}-n+1})} \right| \quad (15)$$

346 A minimum of three points ($n = 3$) was considered for steady state. In this case, $\hat{E}(n = 3)$ is
 347 usually small and results from measurement uncertainty. When more points are selected, a part of
 348 transient state is included that diverts from the steady-state straight line. In particular, the largest
 349 error is obtained when all the points ($n = N_{tot}$) are considered for estimating the regression line.
 350 Therefore, $\hat{E}(n)$ defines an increasing function. We selected the first value of n for which $\hat{E}(n) \geq$
 351 E , where E is a given threshold that in this study was fixed at 2% (Bagarello et al., 1999). The
 352 transition time was then defined as the corresponding time, $\tau_{crit} = t_{N_{tot}-n+1}$. Transient infiltration

353 conditions were assumed to occur for $0 < t < \tau_{crit}$ (i.e., when $\hat{E} \geq 2\%$). Steady-state conditions were
 354 assumed to exist for $t \geq \tau_{crit}$ (i.e., when $\hat{E} < 2\%$).

355 Once the cumulative infiltration was split into transient and steady states, the SA model was fitted
 356 to each part of the infiltration process. The cumulative infiltration (CI) fitting method (Vandervaere
 357 et al., 2000), that corresponds to non-linear least squares optimization technique, was applied by
 358 fitting Eq.(4a) to the transient stage of infiltration. The quality of the fit was evaluated by
 359 calculating the relative error, Er (%), as suggested by Lassabatere et al., 2006:

$$360 \quad Er = 100 \sqrt{\frac{\sum_{i=1}^k (I_i^{exp} - I_i)^2}{\sum_{i=1}^k (I_i^{exp})^2}} \quad (16)$$

361 where I_i^{exp} and I_i are the experimental and modeled cumulative infiltration for the period of $0 < t <$
 362 τ_{crit} . Next, linear regression analysis of the $I(t)$ data at steady state ($t \geq \tau_{crit}$) was used to estimate the
 363 c_3 and c_4 coefficients of Eq.(4b). Finally, a was calculated by Eq.(6). This iterative procedure is
 364 denoted as criterion EV-CI (V = variable number of data points). We also considered the simpler
 365 case of a regression line defined by the last three points of the cumulative infiltration. The
 366 corresponding method is denoted E3-CI. For these procedures (i.e., EV-VI and E3-CI), we
 367 considered a run to be successful when all coefficients (c_1 , c_2 , c_3 and c_4) were positive since,
 368 according to Eq.(1), they cannot be negative or null. With the aim to give the model the maximum
 369 flexibility in fitting experimental data, the coefficients were left unconstrained, meaning that we did
 370 not constrain c_3 using Eq.(5) in this portion of the analysis (see Table 1).

371 We also attempted to verify the possible existence of a link between the shape of the experimentally
 372 determined infiltration curve and the results of the a calculations. At this aim, we fitted the
 373 empirical Horton (1940) infiltration model to the data:

$$374 \quad I = i_f t + \frac{i_0 - i_f}{k} (1 - e^{-kt}) \quad (17)$$

375 where i_0 ($L T^{-1}$) is the initial infiltration rate ($t = 0$), i_f ($L T^{-1}$) is the final infiltration rate and the
 376 constant k (T^{-1}) determines the rate at which i_0 approaches i_f . This model was chosen instead of
 377 other possible alternatives (e.g. numerical solution of Richards equation) as we target simpler
 378 analytical solutions and practical approaches to solving the infiltration problem. Indeed, it describes
 379 in some detail the complete infiltration curve using only three parameters, and it was found to give a
 380 good representation of the experimentally determined $I(t)$ relationships in other investigations
 381 (Shukla et al., 2003).

382

383 RESULTS AND DISCUSSION

384

385 Analytically generated infiltration data

386 Critical time

387 As an example, **Fig. 1a** shows the analysis conducted by criterion IT-CI for one of the 144 synthetic
388 infiltration runs. Here, the simulation time t_j (corresponding to data points $5 \leq j \leq 45$) was used as
389 the initial assumed value to differentiate between transient and steady-state data. The corresponding
390 $\tau_{crit,j}$ values were then calculated based on the fitted c_1 , c_2 , c_3 , and c_4 coefficients (expressed as a
391 fraction of the optimal value of each coefficient in **Fig. 1b**). The absolute differences between t_j and
392 $\tau_{crit,j}$ shows a clear minimum at $j = 24$. This minimum is close to, but not quite, zero due to the
393 discretization of the $I(t)$ data. All tested experiments showed similar distinct minimum values for $|t_j$
394 $- \tau_{crit,j}|$. Cumulative infiltration for this experiment is shown in **Fig. 1c** with the fitted models
395 Eq.(4a) and Eq.(4b) corresponding to the optimal set of coefficients. The maximum error for this
396 case was $E_{max} = 0.0031$, whereas for the entire dataset ($N = 144$) E_{max} varied between 0.0015 and
397 0.0042, with a mean value of 0.0029 (**Table 3**).

398 The critical time estimated by the criterion IT-CI varied by more than three orders of magnitude: the
399 ratio between the highest and lowest τ_{crit} values was 2650. The IT-CI algorithm resulted in τ_{crit}
400 values that were systematically higher than the values estimated using the IT-CL algorithm (**Table**
401 **3**), with a constant factor of 1.096 between the two. This result confirmed that fitting the transient
402 stage of the infiltration process is a challenging task even with analytical (i.e., error-free) data. As a
403 matter of fact, estimates of c_1 with the two techniques differed by a constant factor of 1.022 and the
404 estimates of c_2 differed by a mean factor of 1.013 (min = 1.006, max = 1.028). In other words,
405 applying the cumulative linearization technique (IT-CL), instead of the non-linear least squares
406 technique (IT-CI), resulted in a relative overestimation of coefficient c_1 and a relative
407 underestimation of c_2 due to the inter-compensation between the two coefficients (Vandervaere et
408 al., 2000). In turn, such differences yielded a different selection of the transient or steady-state data
409 and, consequently, different estimates for both the τ_{crit} and a parameters. Nonetheless, the a values
410 estimated by the two transient fitting techniques were highly correlated ($R^2 > 0.999$) and the
411 criterion IT-CI overestimated a by a mean factor of 1.017 compared to criterion IT-CL (**Table 3**).
412 Moreover, for each combination of soil, ring diameter and initial water saturation, the factor of
413 discrepancy between the estimated a values using the two fitting techniques was in the range of
414 1.008-1.029. Thus, the influence of the fitting technique on the prediction of a can be considered
415 small and probably negligible in practice. For the subsequent analyses, only the results obtained by

416 the non-linear least squares technique (criterion IT-CI) were considered, as that approach was also
417 consistent with the criterion applied for the field data.

418 The analytical data confirmed the proportionality between τ_{crit} and t_{max} , that was theoretically
419 expressed by Eq.(13), for all types of soils. In particular, for the analytical infiltration experiments
420 performed in this study, the ratio τ_{crit}/t_{max} was constant and equal to 1.495, regardless of the
421 combination of soil, ring diameter and initial water saturation (**Fig. 2a**). It is worth noting that this
422 ratio was obtained for $\beta = 0.6$, and may be subject to change as β varies. Also, as stated in the
423 methods section, we tested the sensitivity of a estimates by fixing τ_{crit} at t_{max} . That comparison
424 showed that the two sets of estimated a values were highly correlated but that those values obtained
425 by the iterative criterion (**Fig. 2b**) were larger by a mean factor of 1.02 than those obtained under
426 the assumption of equal characteristic times ($0.71 \leq a \leq 0.90$ with criterion IT-CI and $0.68 \leq a \leq$
427 0.89 with $\tau_{crit} = t_{max}$). This analysis of sensitivity confirmed that t_{max} does not represent an accurate
428 estimate of the transition time of the Stewart and Abou Najm (2018a) model. Nonetheless,
429 differences in the estimation of τ_{crit} up to a factor of 1.5 yielded estimations of a that were
430 practically coincident (i.e., differing from one another by at most a factor of 1.04).

431

432 *Coefficients of the infiltration model*

433 **Fig. 3** summarizes the optimal values of the infiltration model coefficients, c_1 , c_2 , c_3 , c_4 , obtained
434 for each soil, ring diameter and initial soil water saturation. Similarities can be noted between c_1 and
435 c_3 , and again between c_2 and c_4 . Further, c_2 and c_4 are nearly constant regardless of S_e , indicating the
436 importance of K_s relative to the macroscopic capillary length within the factor f (Eq.2), since only
437 the latter will decrease with S_e . The results also show that capillarity is relatively more important in
438 small rings (e.g., $r_d = 40$ mm) compared to large rings (e.g., $r_d = 150$ mm) as a consequence of
439 lateral sorption representing more of the total flow when the ring perimeter is relatively large
440 compared to the ring area. This process means that the values of c_2 and c_4 are higher and the
441 reductions with increasing S_e more evident in the smaller rings compared to the larger ones.

442 At the same time, the c_1 coefficient represents soil sorptivity in these infiltration models, so the
443 reported curves appear physically plausible since they decrease as the initial saturation degree S_e
444 increases. Indeed, we expect sorptivity, i.e. capillarity driven infiltration, to be at its maximum for
445 initially dry soils. Moreover, early time infiltration is governed by vertical capillary-driven flow and
446 does not depend on the 3D flow term; therefore, ring size has no effect on the estimates of the c_1
447 coefficient. It is worth noting that, with the analytically generated cumulative infiltration curves, the
448 coefficient c_3 is also independent of ring size. This result is a consequence of the assumed

449 continuity of the transient and steady-state infiltration curves at the transition time, which is
450 specified by Eq.(5).

451 The meaningful trends of the estimated coefficients (**Fig. 3**), and the consistency with the
452 constraints of the Stewart and Abou Najm (2018a) model, prove that the iteration criterion used for
453 analyzing the synthetic infiltration data was effective in estimating the transition time τ_{crit} and the
454 associated set of coefficients c_1, c_2, c_3, c_4 .

455

456 *a parameter*

457 The results of the iterative criterion were thus used to test the effects of initial water content and
458 ring radius on the a constant of SA model (**Fig. 3, last row**). The a values calculated by Eq.(6),
459 using the infiltration coefficients estimated by the iterative approach IT-CI, varied between 0.706
460 and 0.904, with a mean of $a = 0.807$ (**Table 3**). Therefore, the iterative procedure yielded a
461 parameter values that were, on average, closer to the value suggested by Wu and Pan (1997) than
462 the recommendations of Stewart and Abou Najm (2018a). Soil texture affected the a constant, with
463 the sandy and sandy loam soils having the lowest a values and the silt loam and silty clay loam soils
464 yielding the highest a values. The a parameter decreased as the ring diameter increased and was
465 more influenced by ring size than initial water content.

466 It must be noted that the synthetic infiltration data were obtained by the implicit model developed
467 by Haverkamp et al. (1994) and that those authors suggested using their model only when the initial
468 water content is lower than 0.25 of the saturated water content. Despite this potential limitation, our
469 results show that the value of a remains strictly constant for $S_e < 0.5$, and its value only slightly
470 varied when the initial degree of saturation was in the range $0.5 \leq S_e \leq 0.8$. Therefore, the
471 simplification presented in Eq.(9), which suggests that a depends only on ring size and soil
472 properties such as λ_{max} and K_s , appears to be valid for a fairly wide range of initial water contents.

473

474

475 **Field experiments**

476 The average duration of the 60 infiltration tests was of 0.78 h ($CV = 105.6\%$). Application of the
477 most rigorous criterion, IT-CI, only succeeded in 25 out of 60 infiltration tests (42% success rate).
478 In most cases, failure was due to the lack of a well-defined minimum for the $|t_j - t_{crit,j}|$ function. The
479 successful runs had a mean duration of 0.77 h and a mean τ_{crit} of 0.57 h. The constrained fitting of
480 the infiltration coefficients resulted, in some cases, in low or negative values of c_3 that is the
481 intercept of the regression line fitting the steady-state stage of the infiltration curve (**Table 4**). The
482 25 experiments that were successfully treated with the IT-CI criterion yielded a mean a value of

483 0.883 ($CV = 26.1\%$). Calculated a values were implausible in 5 out of 25 successful runs (i.e., $a >$
484 1). Excluding these values from the analysis yielded a mean value $a = 0.783$ ($CV = 14.5\%$, $N = 20$)
485 (**Table 4**).

486 As explained in the methods section, we also tested two empirical criteria as simpler methods for
487 estimating the transition time: E3-CI and EV-CI. An example of these two fitting procedures is
488 shown in **Fig. 4**. When we used the E3-CI criterion, 44 out of 60 infiltration tests were successfully
489 fitted (i.e., positive infiltration coefficients), representing a success rate of 73%. The successful runs
490 had a mean duration of 0.96 h and a mean τ_{crit} of 0.58 h, while the unsuccessful runs had a mean
491 duration of 0.31 h and a mean τ_{crit} of 0.19 h. Application of the more flexible criterion for assessing
492 the steady-state (i.e., criterion EV-CI) resulted in a similar success rate, as estimation succeeded in
493 43 out of 60 cases (72% success rate). The number of cumulative infiltration data defining the
494 steady-state infiltration stage ranged from a minimum of 9 to a maximum of 15. The successful runs
495 had a mean duration of 0.98 h and a mean τ_{crit} of 0.44 h, while the unsuccessful runs had a mean
496 duration of 0.30 h and a mean τ_{crit} of 0.16 h.

497 Reasons of failure included obtaining $c_1 = 0$ (9 cases for E3-CI and 10 cases for EV-CI), $c_1 = 0$ and
498 $c_3 < 0$ (4 cases with both E3-CI and EV-CI), and $c_2 = 0$ (3 cases with both E3-CI and EV-CI). We
499 note that the iterative criterion (IT-CI) also failed for all of the aforementioned infiltration runs,
500 leading to the conclusion that estimating the transition time can identify tests that do not follow
501 theory, regardless of the applied criterion. The $c_2 = 0$ results were associated with high c_1 values ($>$
502 $440 \text{ mm/h}^{0.5}$), i.e., high apparent soil sorptivity (**Fig. 5**, points located on the y-axis). On the other
503 hand, $c_1 = 0$ results were associated with high c_2 values ($> 600 \text{ mm/h}$), i.e., high apparent saturated
504 conductivity (**Fig. 5**, points located on the x-axis). These two extreme scenarios are typical of two
505 opposite types of soils, i.e., fine soils prone to capillarity-driven flow on one hand, and coarse soils
506 prone to gravity-driven flow on the other. Experimental runs thus confirmed that possible inter-
507 compensation between the coefficients c_1 and c_2 may complicate fitting of the transient infiltration
508 relationship. **Fig. 6** shows an example of the cumulative infiltration curve for each reason of failure.
509 In short, runs failed when i) I was nearly linear with t (lack or very short duration of an initial
510 transient phase, **Fig. 6a**) (Angulo-Jaramillo et al., 2019), ii) the infiltration rates increased with
511 time, as expected in water repellent soil conditions (**Fig. 6b**) (Beatty and Smith, 2013; Ebel and
512 Moody, 2013), and iii) concavity was or appeared to be particularly pronounced, as for sealing soils
513 (Di Prima et al., 2018) (**Fig. 6c**).

514 Criterion E3-CI, being based on the last three cumulative infiltration data, generally yielded higher
515 τ_{crit} values compared to criterion EV-CI, which estimated the steady-state infiltration from a larger
516 dataset (**Fig. 4**). According to criterion E3-CI, the mean τ_{crit} value was equal to 0.47 h ($CV =$

517 100.3%). When criterion EV-CI was used to estimate the steady-state stage of the infiltration
518 process, the mean τ_{crit} was 0.36 h ($CV = 93.8\%$), i.e., 18% lower than the mean critical time
519 estimated by criterion E3-CI. In both cases, the critical time increased with the duration of the run
520 (**Fig. 7**).

521 Despite the different estimates of the transition time, the two empirical criteria (E3-CI and EV-CI)
522 were almost equivalent in estimating the coefficients c_1 , c_2 , c_3 and c_4 of Eq.(4) as showed by the
523 high values of the correlation coefficient ($0.936 \leq r^2 \leq 0.997$). In particular, selecting a longer
524 steady-state interval, as per criterion EV-CI, resulted in the estimates for coefficient c_3 that were
525 lower than those of the E3-CI method by a mean factor of 1.18 (**Table 4**). Conversely, coefficient c_4
526 attained using EV-CI was larger by a mean factor of 1.07 than those of E3-CI. The field data thus
527 confirmed the results obtained with analytical data, specifically that differences when identifying
528 the relative duration of transient versus steady-state infiltration stages had minor influence on
529 estimated infiltration coefficients.

530 We did not impose a constraint for coefficient c_3 for either empirical criteria (i.e., E3-CI and EV-
531 CI), because in both cases the transition time was assumed a-priori and independently from the
532 fitted infiltration coefficients. This simplification implies that the fitted cumulative infiltration curve
533 may be discontinuous for $t = \tau_{crit}$. As a matter of fact, for the 43 successful runs with both criteria,
534 the estimates of I calculated for $t = \tau_{crit}$ with the transient (Eq.4a) and the steady-state (Eq.4b)
535 models differed by a percentage ranging from -6.6% to 2.9%. The fitting algorithms therefore
536 identify parameter values that can vary from the theoretical constraints placed by the SA model.
537 Nonetheless, these results still show that the tested empirical algorithms are sufficiently reliable to
538 interpret field measurements, with the specific advantage of being simpler to apply compared to
539 iterative criterion.

540 At the same time, it is likely that the unconstrained c_3 values had little or no influence on the
541 calculations of the a constant, as that term was estimated only with the c_2 and c_4 coefficients. The
542 valid infiltration runs yielded a values varying from 0.239 to 1.690. The null hypothesis that the
543 positive a values were normally distributed was not rejected (Lilliefors 1967 test; $\alpha = 0.05$);
544 consequently, the a values were summarized by the arithmetic mean and the associated CV (**Table**
545 **4**).

546 For the 44 runs that yielded positive a results with criterion E3-CI, the relative error of the transient
547 infiltration model, Er , was $\leq 6.1\%$ (mean = 2.2%). In addition, Er was less than 3.5% in the 86.4%
548 of the cases, denoting a good fit of the model to the data considering a threshold of 5% as suggested
549 by Lassabatere et al. (2006). For the 43 runs that yielded positive a results with criterion EV-CI, Er
550 was $\leq 3.8\%$ (mean = 1.7%), thus denoting a better fitting of the model as compared to criterion E3-

551 CI. Nonetheless, the a values obtained by the two approaches (E3-CI and EV-CI) differed by a
552 nearly negligible mean factor of 1.10 (**Table 4**) and were significantly correlated ($R^2 = 0.997$).

553 However, a rather high percentage of calculated a values were implausible, as 20 out of 44
554 individual values were > 1 with criterion E3-CI (i.e., 45% of tests). An even larger percentage of
555 physically implausible values (i.e., $a > 1$) were obtained by criterion EV-CI (55% of tests).

556 Excluding values of $a > 1$ from the analysis, the mean a parameter values were similar between
557 criteria: $a = 0.735$ for E3-CI and $a = 0.737$ for EV-CI. The CV of the individual estimates of $a < 1$
558 (27.9%-32.3%) was much lower than the CV s of c_2 and c_4 (**Table 4**).

559 Altogether, the results of this field investigation were consistent with the analysis of the analytically
560 generated infiltration data, since in both cases a was intermediate between the values suggested by
561 Stewart and Abou Najm (2018a), i.e., $a = 0.45$, and Wu and Pan (1997), i.e., $a = 0.91$. However, the
562 field experiments only led to successful a estimates in a limited number of cases. Specifically, 20
563 out of 60 tests (33%) were successful and had physically plausible a values when using IT-CI, 20
564 out of 60 tests were successful and plausible for EV-CI (33%) and 24 out of 60 tests were
565 successful and plausible for E3-CI (40%). Implausible estimates of a could indicate infiltration tests
566 that violates the model assumptions (i.e., homogeneous soil with uniform initial water content) or
567 unsatisfactory description of the steady-state stage with the empirical criterion. In these cases, a
568 practical recommendation could be to fix a at a value close to the maximum theoretical value ($a =$
569 1) and proceed with a constrained estimation of the infiltration coefficients linear with time.

570 The Horton model was successfully fitted to the data for 52 out of the 60 infiltration experiments,
571 and all failures occurred at the AR site. The Er values varied from 0.41 to 4.5% and were lowest at
572 the AR site and highest at the RO site (**Table 5**). For the 44 infiltration runs yielding an estimate of
573 the a constant by the criterion E3-CI, a scattered but rather clear relationship was detected between
574 a and k/i_f ($R^2 = 0.659$), representing a normalized k constant (**Fig. 8**). For these runs, the k/i_f ratio
575 varied between 0.011 and 0.067 mm^{-1} . For the 16 cases in which estimation of a failed, the Horton
576 model was not applicable (eight runs) or k/i_f was either greater than 0.067 mm^{-1} (4 runs) or smaller
577 than 0.011 mm^{-1} (three runs). In a single case, an estimate of a was not obtained, even though k/i_f
578 equaled 0.025 mm^{-1} (and therefore was in the range 0.011-0.067 mm^{-1}). Therefore, the rate at which
579 the initial infiltration rate approached the final infiltration rate, expressed by normalized k constant,
580 explained both variability of a and the success or the failure of the experiment. According to the
581 fitted relationship of **Fig. 8**, obtaining $a < 1$ requires a normalized k constant of more than 0.02 mm^{-1} .

582
583

584 CONCLUSIONS

585 Applying the comprehensive infiltration model by Stewart and Abou Najm (SA model) requires
586 estimating the transition time from transient to steady-state flow conditions, τ_{crit} , and choosing a
587 value for the so-called a constant. In previous tests of the SA model, τ_{crit} was estimated by an
588 empirical criterion based on the premise that the last three infiltration data points describe steady-
589 state conditions, yet that approach had not been rigorously analyzed. Further, the SA model
590 included a recommendation to fix a at a constant value of 0.45, half of the value ($a = 0.91$) that had
591 been proposed in earlier studies. These differences in assumed values for a can affect the model
592 performance, particularly when it is used to estimate soil hydraulic properties from infiltration tests.
593 Given these uncertainties, this investigation introduced a novel, iterative method for estimating τ_{crit}
594 that includes the constraint that the same cumulative infiltration has to be obtained at the time $t =$
595 τ_{crit} with the transient and steady-state explicit expressions of the model. The new estimating
596 criterion of τ_{crit} is physically more robust than the existing estimating criterion since it does not
597 require any a-priori assumptions about the number of data points associated with steady-state
598 conditions. Instead, the new method was shown to fail if steady-state was not reached by the end of
599 the infiltration run, meaning that the method is a valid and useful test of whether infiltration data
600 can accurately be partitioned into transient and steady-state phases. Our tested algorithms all
601 generated slightly different estimates for transition times for the same infiltration data, thus
602 revealing some minor uncertainty associated with these methods. Nonetheless, the differences were
603 for the most part minor, even when using relatively simple fitting algorithms, suggesting that
604 empirical fitting methods are suitable in many instances.

605 This investigation also demonstrated that the a term of the SA model is not a constant and can
606 plausibly vary over the $0.47 < a < 1$ range. The a parameter tends to be larger when small water
607 sources are used and for finer soils. Our analysis, which relied on comparing two parameters that
608 were generated from the transient and steady-state infiltration phases, also determined some a
609 values > 1 . These results are physically implausible, and suggest that in those runs the infiltration
610 phases may not have been accurately demarcated. In such instances, practitioners may consider
611 fixing a at a high but theoretically plausible value (e.g., $a = 0.91$ or 0.95) and then adjusting the
612 other model parameters as necessary. At the same time, this investigation demonstrated that a does
613 not depend appreciably on the applied method to obtain τ_{crit} . In other words, some uncertainty in the
614 estimate of τ_{crit} does not have a relevant impact on estimation of a . These findings together expand
615 the applicability of the SA model by showing that a does not need to be fixed a-priori.

616 The methods for obtaining τ_{crit} and a developed here reveal valuable linkages between theory and
617 practice. Specifically, infiltration tests for which the τ_{crit} estimating method fails or the fitted a

618 parameter exceeds the range of the admissible values can indicate non-ideal infiltration conditions.
619 In these instances, analytical solutions such as the SA model will likely not provide satisfactory
620 descriptions of the processes at work (e.g., non-ideal behaviors related to water repellency or
621 heterogenous flow). In contrast, infiltration runs that result in appropriately constrained τ_{crit} and a
622 values are likely to yield more accurate estimates for soil hydraulic properties, such as saturated soil
623 hydraulic conductivity, when applying the SA model. Therefore, we suggest that this investigation
624 has practical relevance, and that the findings presented here should form the basis of future work
625 aimed at the theory and application of infiltration processes. In particular, carefully controlled
626 experiments should be carried out on other soils to verify that the methods developed here can
627 distinguish between successful and unsuccessful runs under various conditions.

628

629 **ACKNOWLEDGEMENTS**

630 Authors wish to thank N. Auteri for conducting infiltration experiments at RO site.

631

632 **REFERENCES**

633

- 634 Angulo-Jaramillo, R., Bagarello, V., Di Prima, S., Gosset, A., Iovino, M., Lassabatere, L., 2019.
635 Beerkan Estimation of Soil Transfer parameters (BEST) across soils and scales. *Journal of*
636 *Hydrology* 576, 239-261.
- 637 Angulo-Jaramillo, R., Bagarello, V., Iovino, M., Lassabatere, L., 2016. *Infiltration Measurements*
638 *for Soil Hydraulic Characterization*. Springer International Publishing, Cham, pp. 383 pp.
- 639 Bagarello, V., Di Prima, S., Iovino, M., 2017. Estimating saturated soil hydraulic conductivity by
640 the near steady-state phase of a Beerkan infiltration test. *Geoderma* 303(Supplement C), 70-
641 77.
- 642 Bagarello, V., Iovino, M., D. Reynolds, W., 1999. Measuring Hydraulic Conductivity in a Cracking
643 Clay Soil Using the Guelph Permeameter. *Transactions of the ASAE* 42(4), 957-964.
- 644 Bagarello, V., Iovino, M., Lai, J., 2019. Accuracy of Saturated Soil Hydraulic Conductivity
645 Estimated from Numerically Simulated Single-Ring Infiltrations. *Vadose Zone J* 18(1),
646 180122.
- 647 Beatty, S.M., Smith, J.E., 2013. Dynamic soil water repellency and infiltration in post-wildfire
648 soils. *Geoderma* 192, 160-172.
- 649 Bouma, J., 1982. Measuring the Hydraulic Conductivity of Soil Horizons with Continuous
650 Macropores. *Soil Sci Soc Am J* 46(2), 438-441.
- 651 Carsel, R.F., Parrish, R.S., 1988. Developing Joint Probability-Distributions of Soil-Water
652 Retention Characteristics. *Water Resour Res* 24(5), 755-769.
- 653 Di Prima, S., Castellini, M., Abou Najm, M.R., Stewart, R.D., Angulo-Jaramillo, R., Winiarski, T.,
654 Lassabatere, L., 2019. Experimental assessment of a new comprehensive model for single
655 ring infiltration data. *Journal of Hydrology* 573, 937-951.
- 656 Di Prima, S., Lassabatere, L., Bagarello, V., Iovino, M., Angulo-Jaramillo, R., 2016. Testing a new
657 automated single ring infiltrometer for Beerkan infiltration experiments. *Geoderma*
658 262(Supplement C), 20-34.
- 659 Di Prima, S., Rodrigo-Comino, J., Novara, A., Iovino, M., Pirastru, M., Keesstra, S., Cerdà, A.,
660 2018. Soil Physical Quality of Citrus Orchards Under Tillage, Herbicide, and Organic
661 Managements. *Pedosphere* 28(3), 463-477.

662 Dohnal, M., Vogel, T., Dusek, J., Votrubova, J., Tesar, M., 2016. Interpretation of ponded
663 infiltration data using numerical experiments. *Journal of Hydrology and Hydromechanics*
664 64(3), 289-299.

665 Ebel, B.A., Moody, J.A., 2013. Rethinking infiltration in wildfire-affected soils. *Hydrological*
666 *Processes* 27(10), 1510-1514.

667 Haverkamp, R., Ross, P.J., Smettem, K.R.J., Parlange, J.Y., 1994. 3-Dimensional Analysis of
668 Infiltration from the Disc Infiltrometer .2. Physically-Based Infiltration Equation. *Water*
669 *Resour Res* 30(11), 2931-2935.

670 Hinnell, A.C., Lazarovitch, N., Warrick, A.W., 2009. Explicit infiltration function for boreholes
671 under constant head conditions. *Water Resour Res* 45.

672 Horton, R.E., 1940. An approach towards a physical interpretation of infiltration capacity. *Soil*
673 *Science Society of America Proceedings*, 5:399-417.

674 Iovino, M., Abou Najm, M.R., Angulo-Jaramillo, R., Bagarello, V., Castellini, M., Concialdi, P., Di
675 Prima, S., Lassabatere, L., Stewart, R.D., (2021), "Analytical and field data SA model",
676 Mendeley Data, V1, doi: 10.17632/66yxdp2dtn.1

677 Lassabatere, L., Angulo-Jaramillo, R., Soria-Ugalde, J.M., Cuenca, R., Braud, I., Haverkamp, R.,
678 2006. Beerkan estimation of soil transfer parameters through infiltration experiments -
679 BEST. *Soil Sci Soc Am J* 70(2), 521-532.

680 Lassabatere, L., Angulo-Jaramillo, R., Soria-Ugalde, J.M., Šimůnek, J., Haverkamp, R., 2009.
681 Numerical evaluation of a set of analytical infiltration equations. *Water Resources Research*
682 45. <https://doi.org/10.1029/2009WR007941>

683 Latorre, B., Moret-Fernández, D., Lassabatere, L., Rahmati, M., López, M.V., Angulo-Jaramillo,
684 R., Sorando, R., Comín, F., Jiménez, J.J., 2018. Influence of the β parameter of the
685 Haverkamp model on the transient soil water infiltration curve. *J Hydrol* 564, 222-229.

686 Lazarovitch, N., Ben-Gal, A., Šimůnek, J., Shani, U., 2007. Uniqueness of Soil Hydraulic
687 Parameters Determined by a Combined Wooding Inverse Approach. *Soil Sci Soc Am J*
688 71(3), 860-865.

689 Philip, J.R., 1969. Theory of Infiltration. In: V.T. Chow (Ed.), *Advances in Hydrosience*. Elsevier,
690 pp. 215-296.

691 Philip, J.R., 1990. Inverse solution for one-dimensional infiltration, and the ratio A/K1. *Water*
692 *Resour Res* 26(9), 2023-2027.

693 Reynolds, W., Elrick, D., 2002. 3.4.1.1 Principles and parameter definitions. In: J.H. Dane, G.C.
694 Topp (Eds.), *Methods of Soil Analysis, Part 4, Physical Methods*. Soil Sci. Soc. Am.,
695 Madison, Wisconsin, USA, pp. 797–801.

696 Reynolds, W.D., Elrick, D.E., 1990. Ponded Infiltration from a Single Ring .1. Analysis of Steady
697 Flow. *Soil Sci Soc Am J* 54(5), 1233-1241.

698 Russo, D., Bresler, E., Shani, U., Parker, J.C., 1991. Analyses of infiltration events in relation to
699 determining soil hydraulic properties by inverse problem methodology. *Water Resour Res*
700 27(6), 1361-1373.

701 Shukla, M.K., Lal, R., Unkefer, P., 2003. Experimental evaluation of infiltration models for
702 different land use and soil management systems. *Soil Science*, 168(3): 178-191.

703 Šimůnek, J., Šejna, M., van Genuchten, M. Th., 2018. New features of the version 3 of the
704 HYDRUS (2D/3D) computer software package. *Journal of Hydrology and Hydromechanics*,
705 66(2), 133-142, doi: 10.1515/johh-2017-0050, 2018.

706 Smettem, K.R.J., Parlange, J.Y., Ross, P.J., Haverkamp, R., 1994. 3-Dimensional Analysis of
707 Infiltration from the Disc Infiltrometer .1. A Capillary-Based Theory. *Water Resour Res*
708 30(11), 2925-2929.

709 Smiles, D., Knight, J., 1976. A note on the use of the Philip infiltration equation. *Soil Research*
710 14(1), 103-108.

711 Smith, R.E., Smettem, K.R.J., Broadbridge, P., Woolhiser, D.A., 2002. *Infiltration Theory for*
712 *Hydrologic Applications*. American Geophysical Union, Water Resources Monograph.

713 Stewart, R.D., Abou Najm, M.R., 2018a. A Comprehensive Model for Single Ring Infiltration I:
714 Initial Water Content and Soil Hydraulic Properties. *Soil Sci Soc Am J* 82(3), 548-557.
715 Stewart, R.D., Abou Najm, M.R., 2018b. A Comprehensive Model for Single Ring Infiltration II:
716 Estimating Field-Saturated Hydraulic Conductivity. *Soil Sci Soc Am J* 82(3), 558-567.
717 van Genuchten, M.T., 1980. Closed-form equation for predicting the hydraulic conductivity of
718 unsaturated soils. *Soil Sci Soc Am J* 44(5), 892-898.
719 Vandervaere, J.-P., Vauclin, M., Elrick, D.E., 2000. Transient Flow from Tension Infiltrometers I.
720 The Two-Parameter Equation. *Soil Sci. Soc. Am. J.* 64(4), 1263-1272.
721 White, I., Sully, M.J., 1987. Macroscopic and microscopic capillary length and time scales from
722 field infiltration. *Water Resour Res* 23(8), 1514-1522.
723 Wu, L., Pan, L., 1997. A Generalized Solution to Infiltration from Single-Ring Infiltrometers by
724 Scaling. *Soil Sci. Soc. Am. J.* 61(5), 1318-1322.
725 Wu, L., Pan, L., Mitchell, J., Sanden, B., 1999. Measuring Saturated Hydraulic Conductivity using
726 a Generalized Solution for Single-Ring Infiltrometers. *Soil Sci. Soc. Am. J.* 63(4), 788-792.

727

FIGURE CAPTIONS

728
729
730
731
732
733
734
735
736
737
738
739
740
741
742
743
744
745
746
747
748
749
750
751
752
753
754
755
756
757
758
759
760
761

Figure 1. Example of application of iterative criterion IT-CI. In a) the values for t_j , $\tau_{crit,j}$, and the absolute difference between the two, $|t_j - \tau_{crit}|$, are calculated for each data point j between 5 and 45. In b) the estimated parameters c_1 , c_2 , c_3 , and c_4 are expressed as fractions of the optimal value for each parameter, $c_{i,opt}$. In c) cumulative infiltration is modelled using Eq.(4) with the optimal set of parameters; the white dot shows the transition time.

Figure 2. Comparison between a) transition time τ_{crit} and maximum time t_{max} for the analytically generated infiltration experiments; b) values of a constant estimated by the iterative criterion IT-CI and assuming $\tau_{crit} = t_{max}$

Figure 3. Optimized coefficients c_1 , c_2 , c_3 and c_4 and a parameter as a function of initial degree of saturation, S_e , obtained for each soil and ring radius, r_d , by the iterative criterion IT-CI applied to analytically generated infiltration data.

Figure 4. Example of τ_{crit} estimation by different approaches for identifying the steady-state stage of the infiltration process. Criterion E3-CI considers regression line fitting the last three data points. Criterion EV-CI considers regression line fitting the whole set of cumulative infiltration data for which $\hat{E} \leq 2\%$ (Eq.(14)).

Figure 5. Scatter plot of the c_1 vs. c_2 coefficients estimated by criteria EV-CI (crosses) and E3-CI (circles). (sample size, $N = 60$)

Figure 6. Examples of unsuccessful runs: a) $c_1 = 0$; b) $c_1 = 0$ and $c_3 < 0$; and c) $c_2 = 0$. Blue lines indicate the fitting of the transient model to the data and red lines indicate the adaption of the steady-state model to the data

Figure 7. Relationship between the total duration of the field run and the τ_{crit} time estimated by criteria EV-CI (crosses) and E3-CI (circles). (sample size, $N = 60$)

Figure 8. Relationship between the estimated a parameter and the normalized k constant of the Horton infiltration model

762

763 **Table 1.** Characteristics of the different criteria considered in the study for applying the SA model
 764 to analytical (A) or field (F) infiltration data.

Criterion	data	Transient time, τ_{crit} , estimation	Fitting of transient infiltration data	Fitting of steady infiltration data	Parameter a estimation
IT-CI	A, F	Iterative approach with coefficient c_3 constrained by Eq.5	Non-linear least squares technique	Linear regression	$a = c_2/c_4$
IT-CL	A	Iterative approach with coefficient c_3 constrained by Eq.5	Cumulative linearization technique (Smiles and Knight, 1976)		
EV-CI	F	Linear regression line with variable number of steady infiltration data ($E = 2\%$)	Non-linear least squares technique		
E3-CI	F	Linear regression line with 3 steady infiltration data ($E = 2\%$)	Non-linear least squares technique		

765

766

767

768 **Table 2.** Mean and coefficient of variation, CV , of the soil water content, θ_i , and the dry soil bulk
 769 density, ρ_b , at the beginning of the infiltration run (sample size, $N = 10$ for each summarized
 770 dataset)
 771

Site	Date	θ_i (m ³ /m ³)		ρ_b (g/cm ³)	
		mean	CV (%)	mean	CV (%)
AR	November 2017	0.215	6.5	0.966	6.0
	April 2018	0.199	15.3	0.957	11.1
	May 2018	0.137	12.0	0.979	7.9
	September 2018	0.103	11.8	1.037	6.9
	April 2019	0.158	21.8	1.064	5.5
RO	June 2019	0.184	16.1	0.998	7.1

CV = coefficient of variation

772
 773
 774

Table 3. Statistics of infiltration coefficients, transition time, τ_{crit} , parameter a and maximum error of fit for analytically generated infiltration data by optimization criteria IT-CI and IT-CL.

	criterion	c_1 (mm h ^{-0.5})		c_2 (mm h ⁻¹)		c_3 (mm)		c_4 (mm h ⁻¹)		τ_{crit} (h)		IT-CL
		IT-CI	IT-CL	IT-CI	IT-CL	IT-CI	IT-CL	IT-CI	IT-CL	IT-CI	IT-CL	
SAND	min	34.6	35.4	290.9	283.1	3.3	3.2	391.8	392.4	0.04	0.03	0.0
	max	81.2	83.1	589.0	581.2	13.6	13.2	710.7	711.5	0.11	0.10	0.0
	mean	60.5	61.9	420.2	412.8	8.3	8.1	534.0	534.7	0.07	0.06	0.0
	CV (%)	25.5	25.5	28.1	28.6	41.5	41.5	22.3	22.3	35.8	35.8	6.0
LOAMY SAND	min	23.1	23.7	142.5	138.7	2.8	2.7	192.4	192.8	0.06	0.05	0.0
	max	54.7	55.9	290.6	286.7	12.5	12.2	350.4	350.7	0.21	0.19	0.0
	mean	40.7	41.6	205.8	202.1	7.5	7.4	262.7	263.1	0.13	0.12	0.0
	CV (%)	25.7	25.7	28.4	28.9	43.3	43.3	22.4	22.3	39.4	39.4	6.0
SANDY LOAM	min	14.3	14.6	46.2	45.2	3.2	3.1	62.1	62.2	0.20	0.18	0.0
	max	33.8	34.6	105.8	104.6	15.8	15.4	123.9	124.0	0.87	0.80	0.0
	mean	25.2	25.7	71.9	70.8	9.4	9.2	89.6	89.7	0.53	0.48	0.0
	CV (%)	25.7	25.7	31.9	32.4	44.9	44.9	25.7	25.7	42.9	42.9	6.0
LOAM	min	8.3	8.5	12.2	12.0	4.3	4.2	16.3	16.3	1.06	0.97	0.0
	max	19.6	20.0	32.2	31.9	22.5	22.0	36.5	36.5	5.29	4.82	0.0
	mean	14.6	14.9	21.1	20.8	13.3	13.0	25.3	25.3	3.15	2.87	0.0
	CV (%)	25.6	25.6	36.0	36.5	45.9	45.9	30.0	30.0	45.2	45.2	6.0
SILT LOAM	min	6.6	6.7	6.0	5.9	6.0	5.8	7.8	7.8	3.32	3.03	0.0
	max	15.3	15.7	17.3	17.1	31.8	31.1	19.1	19.1	17.26	15.76	0.0
	mean	11.4	11.7	11.0	10.9	18.9	18.4	12.9	12.9	10.26	9.36	0.0
	CV (%)	25.3	25.3	38.8	39.2	45.9	45.9	33.3	33.3	45.6	45.6	6.0
SILTY CLAY LOAM	min	2.5	2.5	0.9	0.9	5.3	5.2	1.2	1.2	18.49	16.87	0.0
	max	5.6	5.7	2.6	2.6	27.4	26.8	2.9	2.9	95.56	87.21	0.0
	mean	4.2	4.3	1.7	1.7	16.4	16.0	2.0	2.0	57.07	52.08	0.0
	CV (%)	24.7	24.7	38.5	38.9	45.2	45.2	32.9	32.9	45.2	45.2	6.0
ALL SOILS	min	2.5	2.5	0.9	0.9	2.8	2.7	1.2	1.2	0.04	0.03	0.0
	max	81.2	83.1	589.0	581.2	31.8	31.1	710.7	711.5	95.56	87.21	0.0
	mean	26.1	26.7	121.9	119.8	12.3	12.0	154.4	154.6	11.87	10.83	0.0
	CV (%)	80.3	80.3	131.3	131.5	58.4	58.4	129.3	129.3	194.9	194.9	7.0

798
799
800
801

Table 4. Statistics of infiltration coefficients and scale parameter a for the successful application of the iterative criterion IT-CI and the empirical criteria EV-CI and E3-CI. Statistics for plausible estimates of parameter a ($a < 1$) are also reported.

	c_1 (mm h ^{-0.5})	c_2 (mm h ⁻¹)	c_3 (mm)	c_4 (mm h ⁻¹)	a	$a < 1$
<i>Criterion IT-CI</i>						
N	25	25	25	25	25	20
min	56.0	7.0	-50.5	63.3	0.444	0.444
max	215.5	1432.2	185.3	1356.8	1.412	0.916
mean	131.3	633.8	2.0	555.2	0.883	0.783
CV(%)	36.2	58.4	3129.5	62.6	26.1	14.5
<i>Criterion EV-CI</i>						
N	43	43	43	43	43	19
min	3.5	19.7	30.3	63.9	0.270	0.270
max	361.3	2957.5	170.1	2556.0	1.690	0.954
mean	141.9	596.3	88.0	535.4	1.016	0.737
CV(%)	58.6	100.5	39.1	90.1	30.3	27.9
<i>Criterion E3-CI</i>						
N	44	44	44	44	44	24
min	38.2	19.4	33.9	60.9	0.239	0.239
max	463.3	2837.6	188.9	2487.4	1.364	0.976
mean	165.8	518.2	103.5	498.7	0.925	0.735
CV(%)	54.6	105.9	34.9	92.7	30.7	32.3

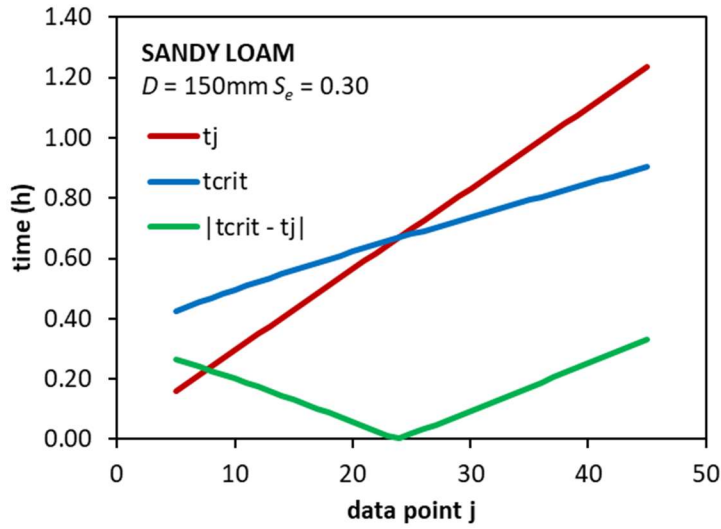
802 N = sample size, Min = minimum value, Max = maximum value, CV = coefficient of variation
803
804
805

806 **Table 5.** Summary statistics of the initial infiltration rate, i_0 , final infiltration rate, i_f , and the
 807 constant k of the Horton infiltration model for each sampled site
 808

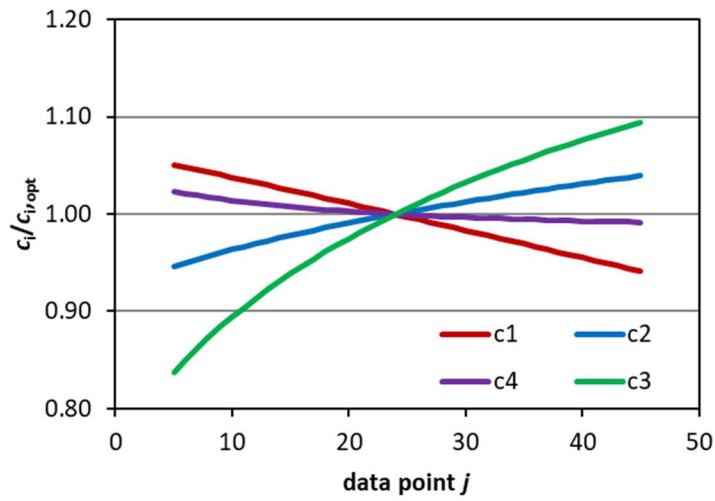
Site	Statistic	i_0 (mm h ⁻¹)	i_f (mm h ⁻¹)	k (h ⁻¹)	Er (%)
AR	N	42	42	42	42
	Min	200.1	9.53	0.093	0.41
	Max	4675.1	1370.2	67.1	4.10
	Mean	1470.0	320.7	8.05	1.29
	Median	1300.0	150.8	3.90	0.99
	CV (%)	62.4	89.6	152.0	61.1
RO	N	10	10	10	10
	Min	416.1	131.0	3.69	1.55
	Max	11243.0	716.1	70.1	4.46
	Mean	2734.2	328.6	19.9	2.89
	Median	890.3	247.5	6.73	2.45
	CV (%)	125.7	55.9	110.7	34.8

809 N = sample size, Min = minimum value, Max = maximum value,
 810 CV = coefficient of variation
 811

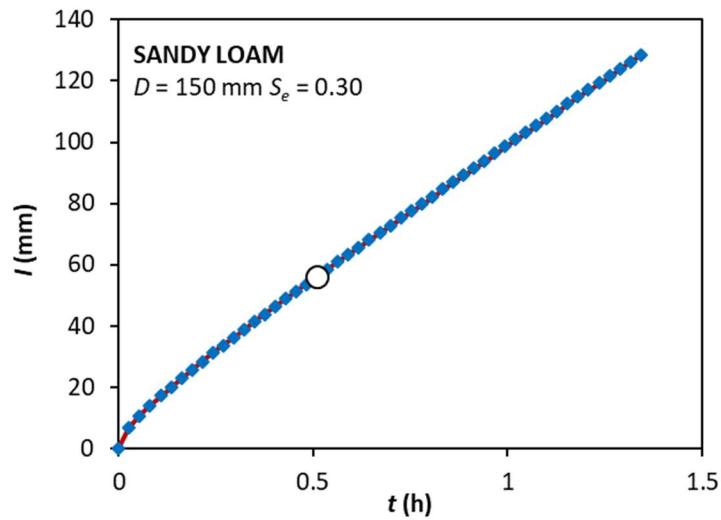
812 **Figure 1.** Example of application of iterative criterion IT-CI. In a) the values for t_j , $\tau_{crit,j}$, and the
 813 absolute difference between the two, $|t_j - \tau_{crit}|$, are calculated for each data point j between 5 and
 814 45. In b) the estimated parameters c_1 , c_2 , c_3 , and c_4 are expressed as fractions of the optimal value
 815 for each parameter, $c_{i,opt}$. In c) cumulative infiltration is modelled using Eq.(4) with the optimal set
 816 of parameters; the white dot shows the transition time.
 817



a)



b)



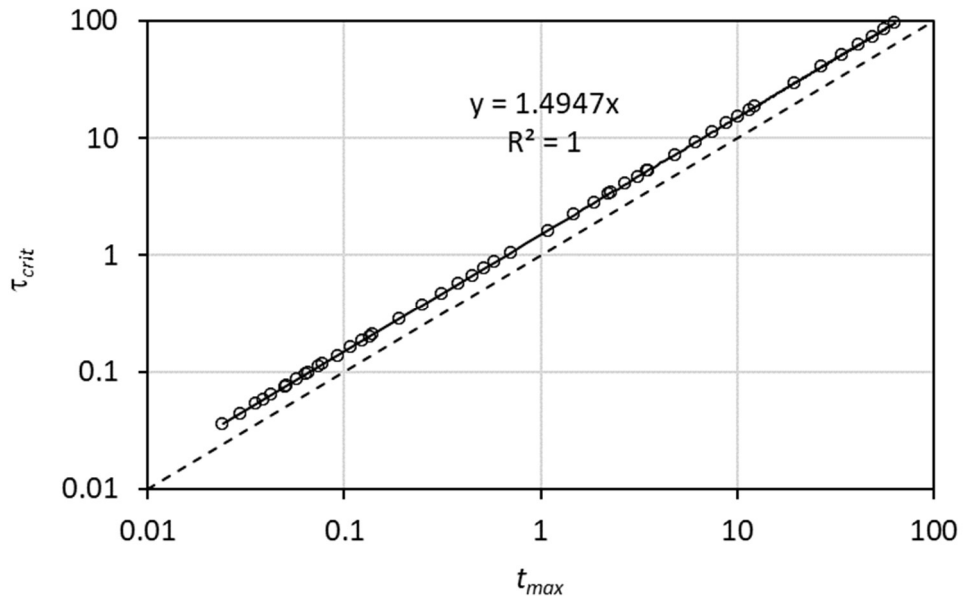
c)

818
819

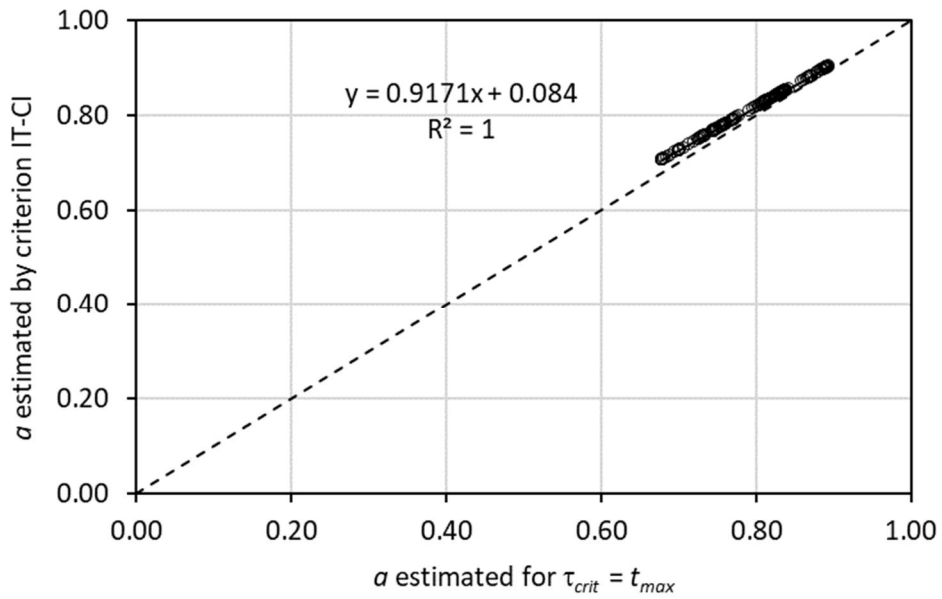
820

821

822 **Figure 2.** Comparison between a) transition time τ_{crit} and maximum time t_{max} for the analytically
 823 generated infiltration experiments; b) values of a constant estimated by the iterative criterion IT-CI
 824 and assuming $\tau_{crit} = t_{max}$
 825



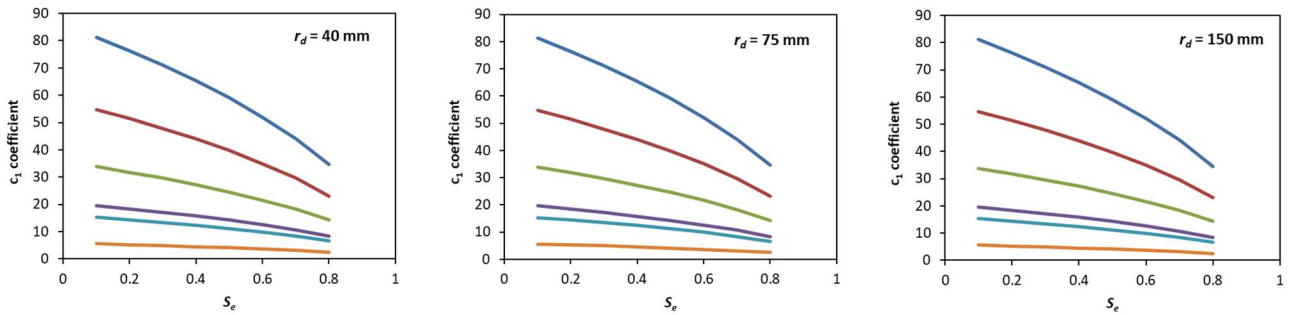
826 a)



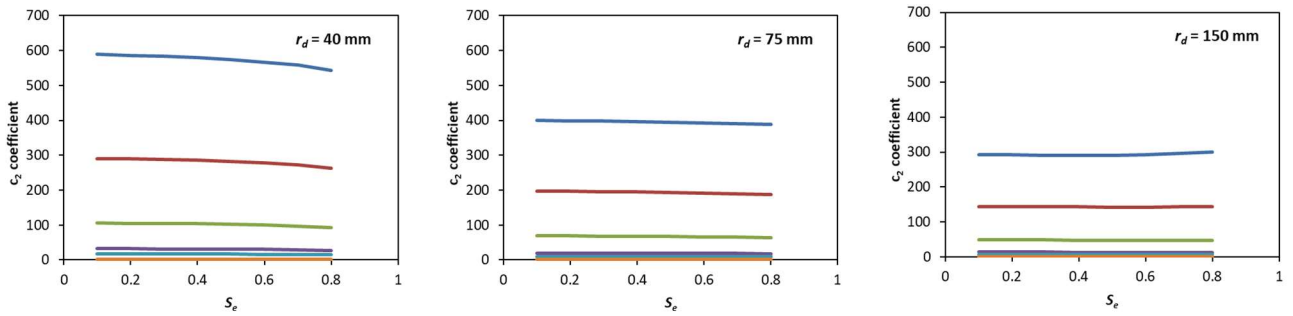
827 b)
 828

829 **Figure 3.** Optimized values of infiltration coefficients c_1 , c_2 , c_3 and c_4 and a parameter as a function
 830 of initial degree of saturation, S_e , obtained for each soil and ring radius, r_d , by the iterative criterion
 831 IT-CI applied to analytically generated infiltration data.
 832

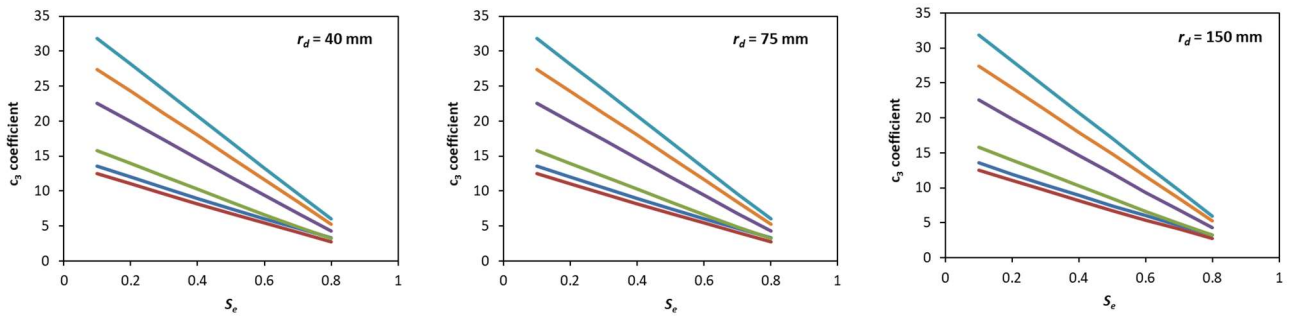
833



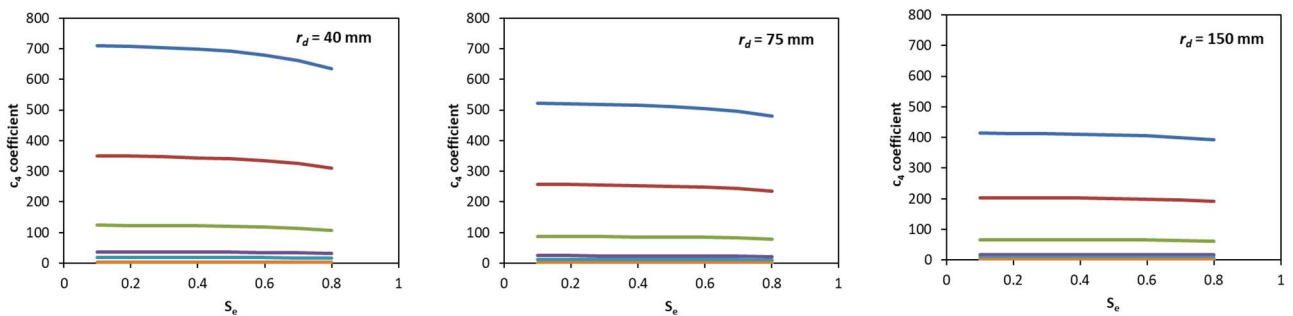
834



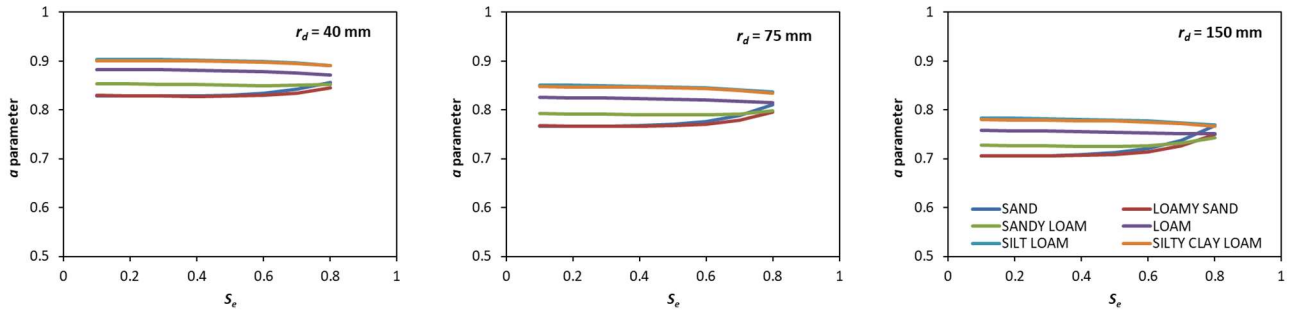
835



836



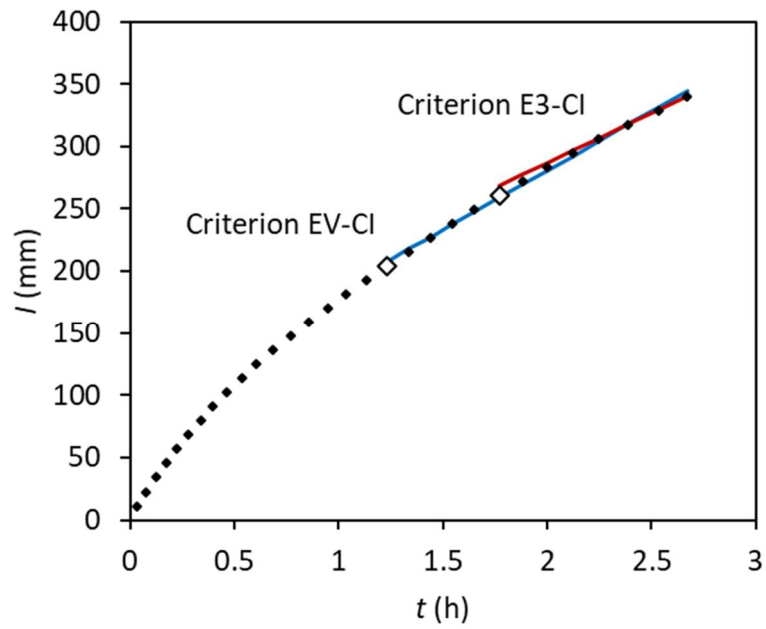
837



838

839

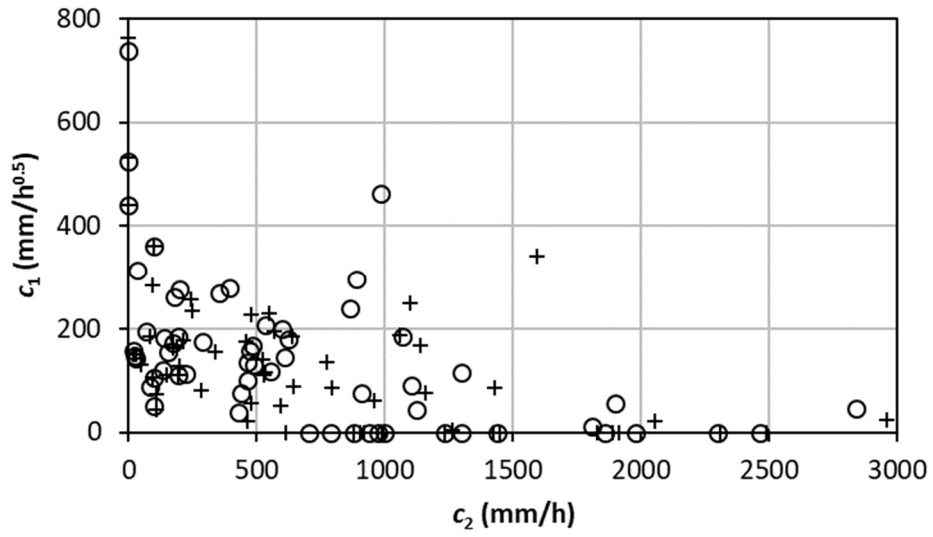
840 **Figure 4.** Example of τ_{crit} estimation by different approaches for identifying the steady-state stage
841 of the infiltration process. Criterion E3-CI considers regression line fitting the last three data points.
842 Criterion EV-CI considers regression line fitting the whole set of cumulative infiltration data for
843 which $\hat{E} \leq 2\%$ (Eq.(14)).
844
845



846

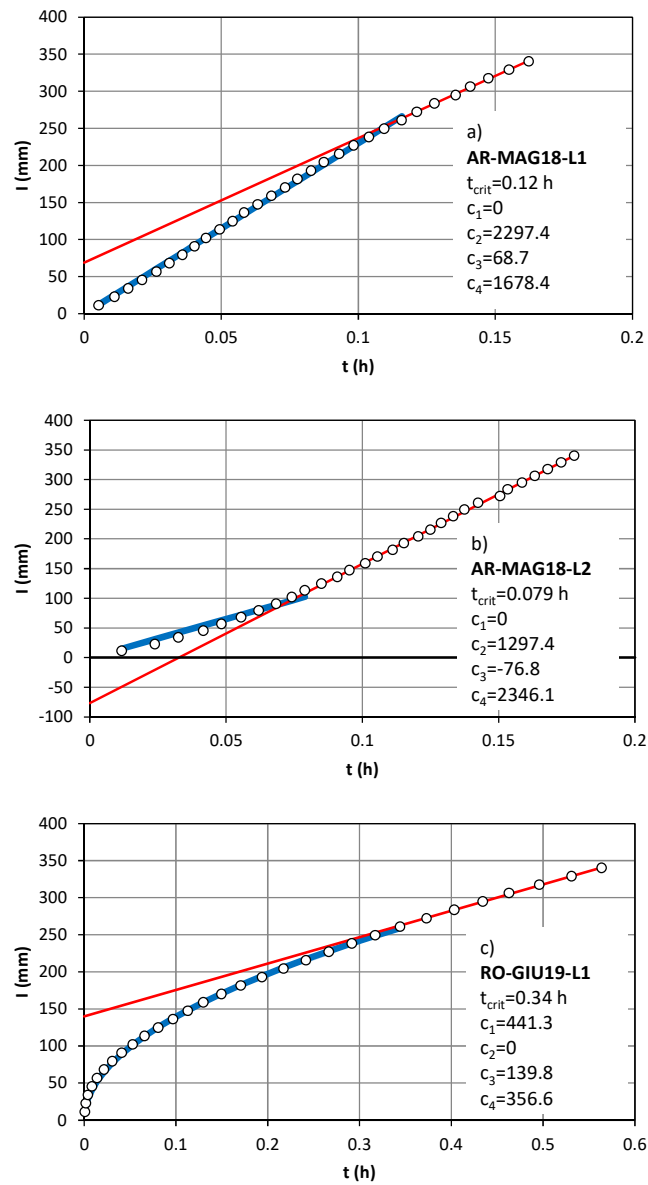
847

848 **Figure 5.** Scatter plot of the c_1 vs. c_2 coefficients estimated by criteria EV-CI (crosses) and E3-CI
849 (circles). (sample size, $N = 60$)
850
851
852



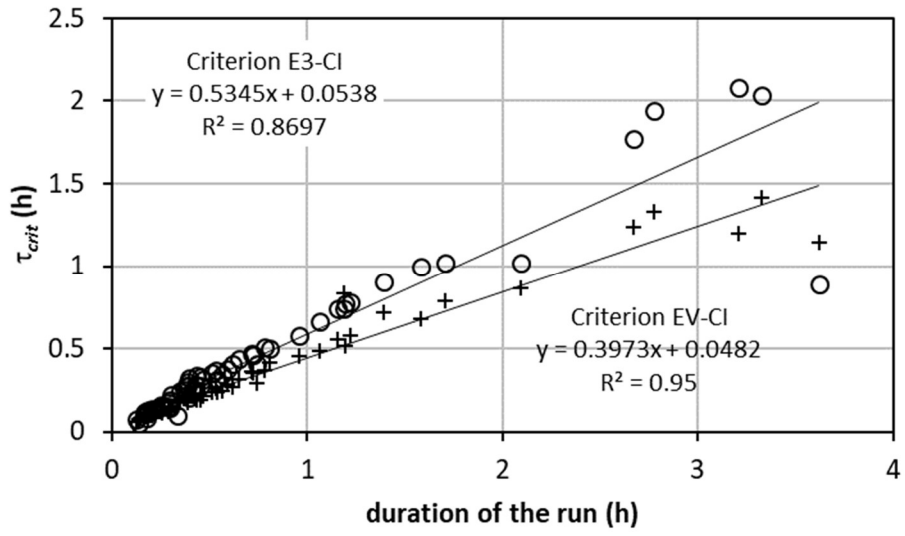
853
854
855
856

857 **Figure 6.** Examples of unsuccessful runs: a) $c_1 = 0$; b) $c_1 = 0$ and $c_3 < 0$; and c) $c_2 = 0$. Blue lines
 858 indicate the fitting of the transient model to the data and red lines indicate the adaption of the
 859 steady-state model to the data
 860



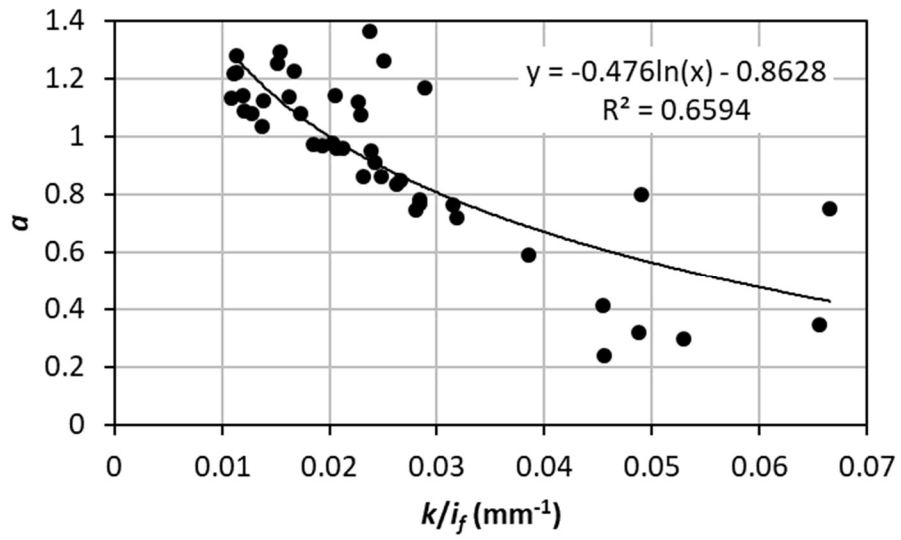
861
 862

863 **Figure 7** Relationship between the total duration of the field run and the τ_{crit} time estimated by
864 criteria EV-CI (crosses) and E3-CI (circles). (sample size, $N = 60$)
865



866
867

868 **Figure 8.** Relationship between the estimated a parameter and the normalized k constant of the
869 Horton infiltration model
870



871

872